Polygonal cracks in the seasonal semi-translucent CO_2 ice layer in Martian polar areas

Ganna Portyankina,[1] Antoine Pommerol,[1] Klaus-Michael Aye,[1] Candice J. Hansen,[2] and Nicolas Thomas[1]

Received 4 August 2011; revised 17 October 2011; accepted 1 December 2011; published 14 February 2012.

[1] In this paper, we use morphological and numerical methods to test the hypothesis that seasonally formed fracture patterns in the Martian polar regions result from the brittle failure of seasonal CO_2 slab ice. The observations by the High Resolution Imaging Science Experiment (HiRISE) of polar regions of Mars show very narrow dark elongated linear patterns that are observed during some periods of time in spring, disappear in summer and re-appear again in the following spring. They are repeatedly formed in the same areas but they do not repeat the exact pattern from year to year. This leads to the conclusion that they are cracks formed in the seasonal ice layer. Some of models of seasonal surface processes rely on the existence of a transparent form of CO_2 ice, so-called slab ice. For the creation of the observed cracks the ice is required to be a continuous media, not an agglomeration of relatively separate particles like a firn. The best explanation for our observations is a slab ice with relatively high transparency in the visible wavelength range. This transparency allows a solid state green-house effect to act underneath the ice sheet raising the pressure by sublimation from below. The trapped gas creates overpressure and the ice sheet breaks at some point creating the observed cracks. We show that the times when the cracks appear are in agreement with the model calculation, providing one more piece of evidence that CO_2 slab ice covers polar areas in spring.

Citation: Portyankina, G., A. Pommerol, K.-M. Aye, C. J. Hansen, and N. Thomas (2012), Polygonal cracks in the seasonal semi-translucent CO_2 ice layer in Martian polar areas, *J. Geophys. Res.*, *117*, E02006, doi:10.1029/2011JE003917.

1. Introduction

1.1. Existence of Translucent CO_2 Ice in Polar Areas of Mars

[2] The Martian polar areas are remarkable for the variety of dynamic seasonal phenomena they exhibit. Every local winter the polar areas of Mars are covered by a CO_2 ice layer. According to Mars Orbiter Laser Altimeter (MOLA) measurements, the maximum thickness of this layer reaches 1.5 and 1.0 m in the north and south polar regions respectively [*Smith et al.*, 2001; *Matsuo and Heki*, 2009]. The seasonal cover consists of solid CO_2 with minor inclusions of water ice and dust [*Leighton and Murray*, 1966]. In this respect the northern and southern seasonal polar caps exhibit a significant difference in that the fraction of water ice is larger in the north than in the south [*Appere et al.*, 2011]. It is the interaction of CO_2 ice sublimation/condensation cycle with the surface and dust and water ice inclusions that leads to the peculiar seasonal activity of Martian polar areas.

[3] The recession of the seasonal polar caps in spring is not symmetric. The most prominent example of an area with unusual properties in the southern seasonal polar cap is the so-called "cryptic region" - an area first defined to lie between latitudes 73°S and 81°S and longitude 175°W–225°W by *Kieffer et al.* [2000]. Thermal Emission Spectrometer (TES) observations [*Kieffer et al.*, 2000] indicated that the cryptic region exhibits an original temporal behavior that is consistent with a coverage by semi-translucent, large grained, solid CO_2 (referred to hereafter as CO_2 slab ice) because of two arguments. First, throughout a vast period in local spring, the temperature of the surface here stays close to the CO_2 sublimation temperature (140 K) although the visible albedo is close to that of bare Martian soil (≃0.3). Second, modeling of TES spectra of the area showed that CO_2 grain sizes in the cryptic region are larger than in other circum-polar areas. Consequently, on the basis of specific CO_2 slab ice properties, Kieffer built a model of sub-ice gas flow [*Kieffer et al.*, 2000]. This model is able to explain formation of several enigmatic features: radially organized channels (now referred to as araneiforms [*Hansen et al.*, 2010]), terrain with lace-like channels, and dark and bright fans. In this model solar energy is able to penetrate through the ice layer to the underlying material, heating it to CO_2 sublimation temperature and starting ice sublimation from the bottom of the layer. Subliming ice creates rising pressure below the ice sheet and eventually breaks through to create cold fountains of CO_2 gas contaminated by some substrate material. For more details on this phenomenon, see *Kieffer* [2007], *Piqueux et al.* [2003],

[1]Physikalisches Institut, University of Bern, Bern, Switzerland.
[2]Planetary Science Institute, Tucson, Arizona, USA.

0148-0227/12/2011JE003917

Hansen et al. [2010], *Thomas et al.* [2010], *Portyankina et al.* [2010], and *Thomas et al.* [2011].

[4] *Piqueux et al.* [2003] showed that the extent and position of the cryptic region varies during spring. For example, there are time periods (from L_s = 175° to 185°) when it covers almost a complete ring around the south pole. At other times it almost completely disappears (from L_s = 195° to 200°). This variability was recently confirmed on small scales by *Pommerol et al.* [2011] using HiRISE and CRISM data. The authors discovered that the top layer of the southern seasonal polar cap undergoes continuous brightening until L_s = 240°–260° (depending on the area). Importantly no correlation with latitude was noted in the available data set. Local substrate properties and topography seem to play a more important role than latitude in the process.

[5] The main result of 2006 OMEGA (Visible and Infrared Mineralogical Mapping Spectrometer onboard Mars Express) observations of the south polar region was that starting from the early beginning of local spring no signature of the exposed surficial slab ice in the cryptic region was observed [*Langevin et al.*, 2006]. Instead OMEGA spectra of the area are consistent with a thin granular layer covering a nearly pure layer of the slab CO_2 ice.

[6] The most recent observations by CRISM are also consistent with the presence of a very thin dust-sand mixture layer on top of the slab ice. This veneer is thick enough to prevent the direct detection of the slab ice in the VIS-NIR range but thin enough to always stay in thermal equilibrium with the underlying CO_2 ice. However these observations provide no indisputable proof of the existence of slab ice [*Brown et al.*, 2010]. The temporal coverage of the southern polar areas by the OMEGA and CRISM instruments is determined by instrument sensitivity and orbit geometry. Very early in spring, i.e., around spring equinox, high-latitude observational conditions for OMEGA and CRISM are not favorable, mainly because of the lack of insolation that results in low signal-to-noise ratios and strong effect of atmospheric aerosols at high incidence angles. Unfortunately, early spring times are considered to be best suited for the creation of ice slab by small particles sintering [*Cornwall and Titus*, 2010]. Some observations show snow transformation toward larger grain sizes which might lead to the slab ice [*Matsuo and Heki*, 2009; *Schmidt et al.*, 2010]. However in the absence of clear spectral information, evidences for the formation of slab ice by the process remain elusive. Direct deposition of CO_2 ice to the surface in the slab form is another possibility. The precise conditions for this however are weakly defined, especially for Martian range of climate conditions. There is still space for speculations if they are met during polar winters or not.

[7] For the model of the formation of fans and araneiforms the question about the existence of the CO_2 slab ice layer remains critical. Particularly important for the plausibility of such a model are the following properties of the slab ice:

[8] 1. It is necessary that the sunlight is able to penetrate the ice slab and deposit energy not only at the top surface, but also to the substrate directly underneath the ice, and perhaps to the impurities inside the ice sheet itself. It is well known that the CO_2 slab ice is extremely transparent [*Hansen*, 1997, 2005]. CO_2 snow on the other hand is very highly scattering. However, depending on the insolation conditions, CO_2 snow, despite increased scattering, might provide enough light to trigger basal sublimation as well [*Pilorget et al.*, 2011].

[9] 2. The ice sheet has to provide enough stability to sustain the pressure growing underneath it for at least some time. Loose snow or firn fail in this task because of extremely low stiffness.

[10] Recent HiRISE observations showed that the northern polar areas also exhibit exotic phenomena that are related to the CO_2 sublimation. Especially active spring sublimation phenomena were observed on the northern polar erg dunes [*Hansen et al.*, 2011]. Fans similar to those in the southern hemisphere and dark spots with alternating bright and dark rings appear over significant areas of the dunes. Mass wasting in the form of the dark streaks was also detected here during local spring in MY29 and 30 [*Hansen et al.*, 2011]. These observations suggest presently active sand transport and dune modification. The possible mechanisms for this dune erosion include sand saltation similar to Earth. Another process involved is Kieffer's model basal CO_2 sublimation [*Kieffer*, 2007]. This triggers the grain flow on the dune slip-faces by entraining surface material from underneath the ice layer and transporting it toward the dune crest. Thus the erosion of Martian dunes could occur with the help of the processes closely related to the one that is thought to be responsible for the araneiform creation.

[11] There has always been less evidence pointing to the existence of the CO_2 slab ice in the northern polar areas. Seasonal CO_2 cover here usually retains a rather high albedo throughout spring which suggests that the top ice layer remains granular. Additions to the surface made up of water (in contrast to the southern hemisphere) and mineral grains obscure spectroscopic signal of CO_2. We have some reasons to expect the CO_2 layer being a slab underneath this top granular layer. One of them is the dune activity described above and the other one is the presence of polygonal cracks that are the topic of this work.

1.2. Seasonal Cracks and Permanent Polygonal Terrains on Mars

[12] Here we report an indirect evidence that the semi-translucent CO_2 ice layer exists in both Martian polar areas for some periods of time during local spring. The analyzed data come from HiRISE onboard MRO [*McEwen et al.*, 2007] and its spectroscopic counterpart, CRISM. We have confirmed with CRISM the presence of some form of CO_2 ice at the surface at the times of HiRISE spring observations. However the interpretation of the spectroscopic signal is ambiguous as the influence of many unconstrained parameters prevents its inversion to a unique physical solution. HiRISE has no spectral capabilities and hence has no possibility to identify CO_2 ice spectroscopically but we have used morphological analysis of its high resolution data to define properties of specific features that can only be explained by the existence of a relatively thick (at least tens of cm) semi-translucent ice slab layer.

[13] The specific features that we have analyzed are elongated dark crack patterns that were observed in the same areas where HiRISE is monitoring early activity of cold jets. In the present paper we argue that these polygonal cracks require a layer of material that (1) is seasonal, (2) forms annually in the same areas, (3) is semi-translucent, and (4) is actively interacting with the top surface layer.

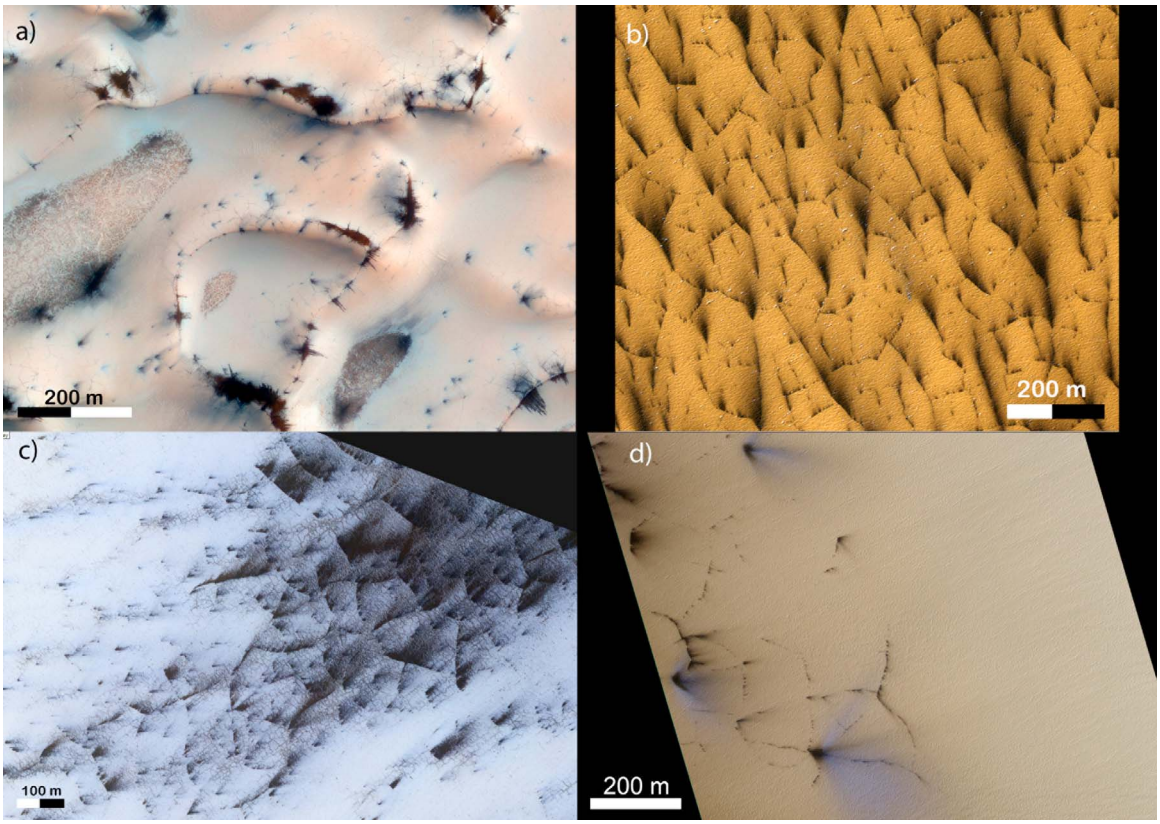

Figure 1. Examples of various polygonal cracks observed by HiRISE in the southern and the northern polar areas. All images are false color images produced by separately stretched infrared, red, and blue-green filters. (a) PSP-008396-2610 - defrosting north polar dunes (81°N, 156°E); (b) ESP-012680-1000- the southern polar terrain (79.9°S, 234.1°E); (c) ESP-012081-0930 - the southern polar terrain (87°S, 72.5°E); (d) PSP-003474-0850 - Giza region (85°S, 69.9°E).

[14] Similar features were also observed and analyzed by *Piqueux and Christensen* [2008] and named "dark polygons". They interpret them as linear vents formed by the sand and dust eruption along "a network of troughs used by the gas as a preferential path during its migration" making a connection between dark polygons of seasonal cap and etched polygonal terrains. However, the authors do not provide a clear explanation for the difference of mechanism between the localized jet activity and activity in the form of "dark polygons". It is important to notice the existence of this particular activity because it provides us with additional important clues about the processes that control the spatial and temporal heterogeneity of jet activity.

[15] The Martian surface is known to exhibit a variety of polygonal terrains. A good overview on this topic can be found in the works of *Levy et al.* [2010] and *van Gasselt et al.* [2005]. Most of Martian polygonal patterns are believed to be thermal contraction cracks (TCC) in ice-rich permafrost [*Mellon*, 1997; *Levy et al.*, 2010], however other types such as desiccation cracks [*Osterloo et al.*, 2007; *El Maarry et al.*, 2010], or lava-related cooling cracks are believed to exist in a number of cases. Morphological criteria for cracks to be identified as TCC were outlined by *Levy et al.* [2009]. Within TCC small-scale polygonal features are fairly common. The scales of cracks that are considered in the present paper fall into the limits for TCC. However, these cracks differ from TCC and the other above mentioned types of cracks in a number of characteristics: (1) they do not show any three-dimensional morphology (elevated polygon interior or raised shoulders, etc.) and are visible as pure albedo features; (2) they are found in polar regions only, at latitudes pole-ward of 70°; (3) they actively change during spring, including scale and intersection type; and (4) they are only observed in spring while TCC remain present during local summer. All these differences allow us to identify an additional type of polygonal cracks with a different physical process creating these. The main characteristic of this new type of cracks is that they are seasonal features in contrast to TCC or desiccation cracks.

[16] Inter-annually changing cracks in a south polar area were previously observed by *van Gasselt et al.* [2005] using Martian Orbital Camera (MOC) images. The cracks were observed in the polar cap trough during two consequent local summers (at L_s = 304–306°) and showed differing patterns. The authors argue that these cracks are situated in a water ice layer that is not completely sublimated at the times of observations. This is supported by surface temperature estimations from the Thermal Emission Spectrometer (TES) that indicate temperatures above those of CO_2 ice. However, the poor spatial resolution of TES leads to averaging the rather different temperatures of terrains inside the polar cap trough and the ones on top of the polar cap. Hence, it can not be excluded that at the times of these MOC observations by *van Gasselt et al.* [2005], CO_2 is still present at the surface,

at least in form of discontinuous patches, therefore the cracks they found could be formed in this CO_2 ice layer and not in the water ice as the authors propose. These cracks then could be the same type of cracks that are discussed in the present paper. To identify with certainty the material in which the cracks have been observed is difficult without dedicated spectroscopic measurements in this particular location, mainly because very specific trough topography might create localized climate conditions favoring either warmer or colder conditions. In contrast to the cracks observed only in the trough, the cracks we describe in the present paper were observed in multiple locations inside the seasonal polar cap and, most importantly, were never observed during local summer.

[17] We propose that the formation of these seasonal cracks is fundamentally different from the model for the creation of TCC and rather closely related to Kieffer's model for araneiform formation via CO_2 ice basal sublimation.

[18] The morphological analysis of surface features with HiRISE images is a powerful tool because of the high spatial resolution of HiRISE (≈0.3 m.) For the set of selected areas of interest HiRISE also provided temporal coverage good enough for monitoring their spring evolution. To date, HiRISE has observed 2 northern springs and at the time of writing (June 2011) is completing the third southern spring observational campaign. In section 2 we report on our observational findings: we describe the morphology and the evolution of the polygonal cracks in the seasonal ice layer and describe several locations where the cracks were observed and their temporal evolution. We use a simple model of the slab ice stability to investigate appearance of the cracks in section 3 and we draw conclusions and discuss applications of our findings to future work in section 4.

2. HiRISE Observations

2.1. Definition and Main General Features of the Cracks

[19] A crack may be defined as a material separation by opening, with the separation distance substantially smaller than the crack length. Dark linear cracks appear in polar areas in local spring. Figure 1 shows several typical examples. The cracks intersect to form a reticulate or polygonal pattern.

[20] Cracks are observed in both north and south polar areas from latitude 72° to 85°. The first spring observations of cracks by HiRISE are at L_s = 70° in the north polar area and L_s = 196° in the south. They often appear close to the areas of fans and araneiforms, i.e., in some of the most seasonally active areas on the polar caps. These fans are commonly believed to be deposits from outbursts of CO_2 gas coming from below the CO_2 ice layer dragging the dust and sand with it [*Kieffer*, 2007; *Thomas et al.*, 2010]. In Figure 1d both dusty and bluish fans can be seen. Sources of fans usually coincide with the cracks and often - with crack junctions.

[21] *Thomas et al.* [2010] reported the existence of extended linear fan sources that they called fissures. We believe that these fissures are indeed cracks that are discussed in this paper. They are simply harder to identify as cracks in the ice because of their strong dust contamination. In Figures 1c and 1d, one can also see that cracks are sources of dust activity. Based on the cold jet hypothesis, the cracks could be explained as actual fractures in the semi-translucent CO_2 slab layer [*Portyankina et al.*, 2010]. Sublimation of the CO_2 ice from underneath the slab creates high pressure which can bend and consequently rupture the slab. Ice is expected to break along straight fractures. The under-ice pressure thus will be released through the fractures. If escaping gas drags some of the underlying substrate material with it, it will make the ice cracks dark and hence visible. Araneiforms are believed to be troughs carved in the substrate by this process. Discussion on how and if araneiforms relate to the cracks can be found in section 2.2.

[22] Crack sizes vary in length from tens of meters to hundreds of meters. Their width is often as small as 1 pixel of the HiRISE image (usually ≈0.5 m). It can not be excluded that where we see incomplete polygonal patterns of cracks some of them are simply so thin that they can not be resolved by HiRISE. The maximum width of cracks never exceeds a few meters. A decrease in crack length is generally observed while spring progresses. We believe that the crack network gets subdivided into smaller scales because the quickly growing pressure and decreasing thickness of the ice itself make it easier to break.

[23] One particular kind of terrain where cracks are often observed are dune fields that get covered by seasonal CO_2 ice. These include dunes inside craters at high latitudes and north polar erg dune fields (an example is in Figures 1a and 2). The cracks on dunes are also associated with fans, but fans do not always come from the cracks. Their spatial correlation suggests a link in their origins. Despite an extensive search for araneiforms (or similar structures) none have so far been reported in the northern hemisphere of Mars. However, the erosion of the dunes by the under-ice gas flow is extensive enough to be observed and is reported to create changes on an annual basis [*Hansen et al.*, 2011].

2.2. Relation to the Underlying Substrate, Permanent Polygonal Terrains and Araneiforms

[24] In order to evaluate if cracks are connected to any features of the underlying substrate, we conducted additional observations during local summer. In summer, after all the CO_2 ice is gone, the substrate does not show any surface signature in the places where the cracks were observed in spring (Figure 3). We observe no araneiforms, no channels, no polygons, and no boulders in summer images of positions where the cracks were observed in spring. This large scale flatness of the area supports uniform slab ice creation. This leads us to the conclusion that seasonal cracks preferably form on flat and smooth substrates and often in the presence of loose material that is able to smoothen out the uneven ground. This loose material becomes visible as fans during spring. With this material being deposited inside the cracks its presence also might be important for rendering them observable.

[25] It is useful to emphasize here that these seasonal cracks are not the same as etched polygons discussed by *Piqueux and Christensen* [2008] or polygonal terrains at midlatitudes. Etched polygons are carved in the substrate (same as araneiforms) and are not seasonal features. *Piqueux and Christensen* [2008] reported that in spring, the etched polygons are being overlayed by the seasonal cracks. An example of the ice cracks and the etched polygonal terrain in

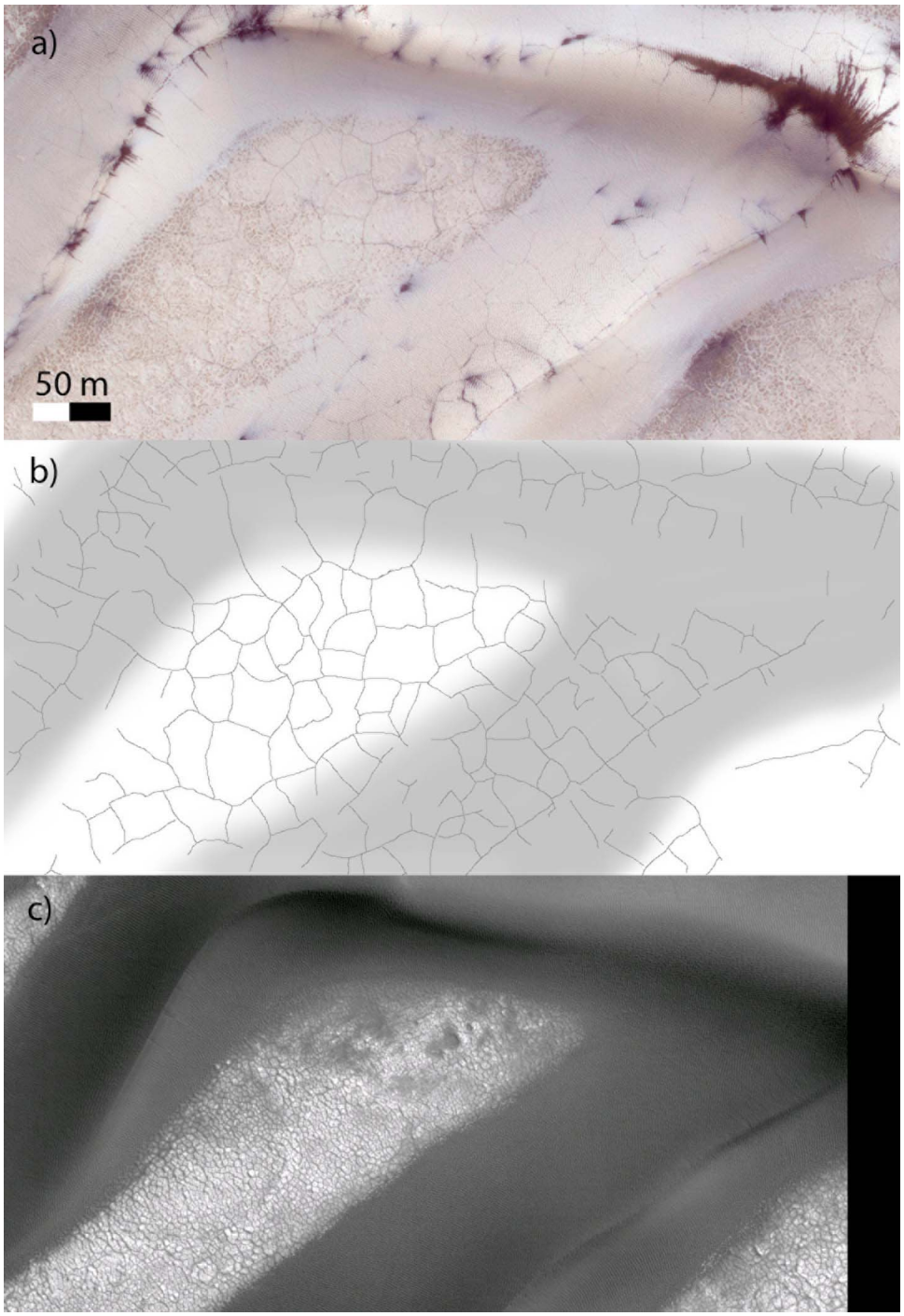

Figure 2. (a) A subsection of HiRISE image PSP-008396-2610 taken during northern spring. The image was taken at L_s = 70.5° at the location 81.0°S, 156.0°E. A thin polygonal crack pattern covers both the dune body and the substrate between the dunes. The pattern is continuous over the separation between dune and substrate providing evidence for existence of the conformal ice cover in the area at this time. (b) Outlined crack positions from the HiRISE image shown in Figure 2a. Grey area indicates position of dune body. (c) HiRISE observation of the same place during local summer (PSP-009398-2610, L_s = 105.0°). Strong albedo contrast between the dune and substrate is visible. No remnants of the crack pattern are present.

the same location is shown in Figure 4. As their orientations and shapes do not mimic each other, we conclude that the seasonal cracks do not form in direct relation to the substrate topography. In the subsequent spring, the cracks form again. They form in the same areas. However their orientations and sizes are not repeated from year to year. One example of this is shown in Figure 5.

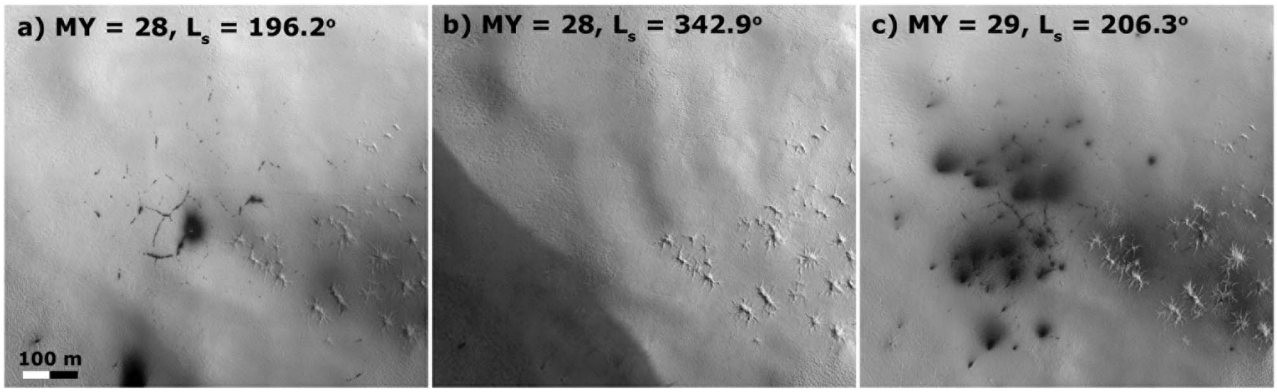

Figure 3. A comparison between HiRISE images (a) PSP-002868-0985 taken during local (southern) spring at L_s = 196.2°; (b) PSP-005993-0985 taken during local summer at L_s = 342.9°; and (c) ESP-011900-0985 taken during spring of the next year at L_s = 206.3°. The location is 81.3°S, 295.8°E.

[26] Araneiforms are topographic features observed exclusively in the southern polar areas: up to 1.5 m deep winding troughs radially converging to a common center. It is interesting to note that the areas where the cracks form, appear smooth and homogeneous and are free of such topographic features. The cracks do not form directly over araneiforms. No matter how close to an araneiform the cracks might appear to be situated they avoid overlying the troughs of araneiforms (see, e.g., Figure 6). If the cracks form under any kind of stress (thermal or mechanical) in the ice layer, this stress should be more easily released over araneiforms. Observations show that araneiform areas tend to be favorable for very early localized jet activity. Our explanation of this is as follows. Their channels provide variability in the surface inclination. The slab ice formed over the flat surface has fewer weakness points compared to where it is draped over highly eroded channeled topography. Additionally small topography variations promote early outgassing activity: some of surfaces are heated more than others because of their orientation toward the sun (which is low at these latitudes and especially at the beginning of spring). In the condition of low solar illumination these surfaces will get significantly larger amounts of energy increasing the probability of starting jets right above araneiforms. The outgassing associated with araneiforms releases pressure from underneath the ice. In the beginning of spring this might be enough to get rid of most pressure underneath large areas and delay cracking of the neighboring flat ice layers. Existing observations of the fan activity indirectly support this: fans over araneiforms usually appear earlier than those coming from the cracks. In the absence of slopes, the CO_2 slab remains intact until very late in the season (L_s = 230–240°). One observed exception to this will be discussed in the next section. Later in the season, the activity over araneiforms diminishes, while the cracks continue to exhibit extensive mobility of dust.

2.2.1. The Cracks in a Context of Global Polar Spring Development

[27] Here we would like to put the appearance and evolution of cracks into the context of the seasonal changes on a larger scale. We will discuss three examples of crack activity in the south polar regions in order to investigate its relationships with the localized jet activity and formulate hypotheses on the control of each type of activity. All the names of areas of interest are carried from previous publications, particularly the works of *Hansen et al.* [2010] and *Pommerol et al.* [2011].

[28] Many works have described the seasonal behavior of polar areas. The asymmetric retreat of the southern seasonal cap and the non-uniform temporal albedo variations were recently discussed by *Pommerol et al.* [2011]. The areas for that investigation were originally selected by their high activity which is mainly defined by the amount of area being covered by fans. In general all examined areas exhibit a surface brightening from L_s = 200° to L_s = 250°. This brightening occurred irrespectively of whether the area was covered by fans at the time, i.e., both fan-covered and fan-free surfaces progressively brightened during this period of time.

[29] Figure 7 shows a rather typical example of development of an area with the ice cracks. The first observed activity is highly localized: many fan-shaped dark deposits appear on the CO_2 covered surface (Figure 7a). Their

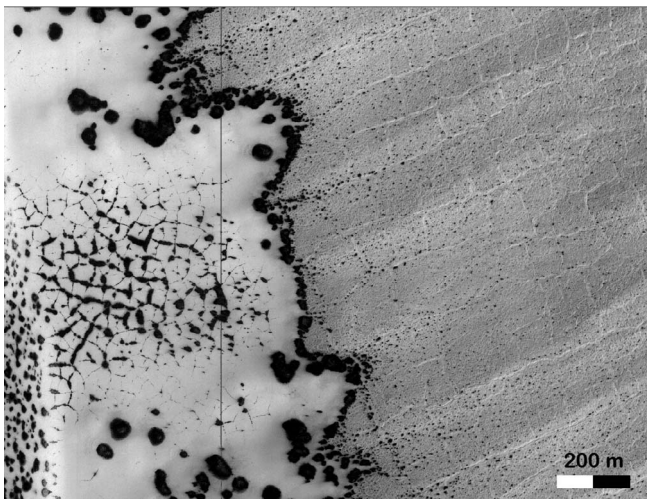

Figure 4. Interaction of the cracks with substrate features: polygonal terrains. The difference of scale and appearance of (left) the cracks in seasonal ice layer and (right) polygonal terrain in 'permanent' substrate layer. Image ESP-012680-1000.

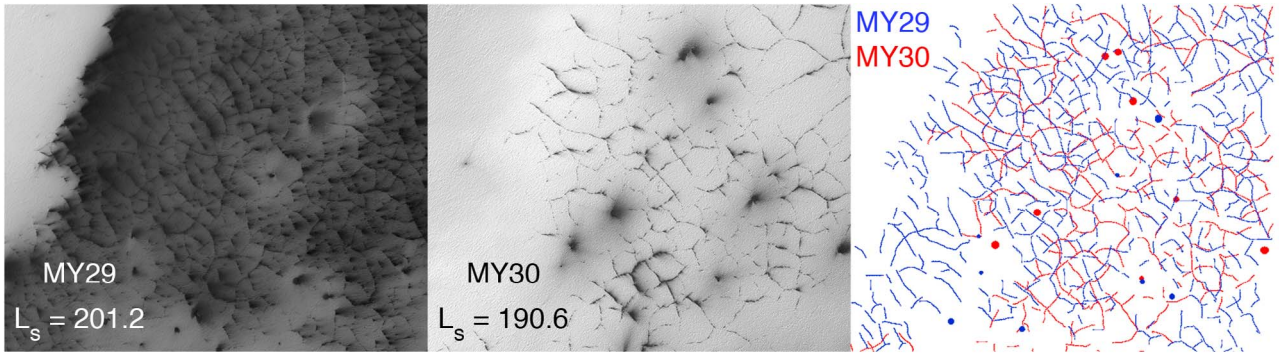

Figure 5. A comparison between (left) HiRISE images ESP-011796-0980 taken during southern spring of Martian year 29 at L_s = 201.2° and (middle) ESP-020376-0980 taken at L_s = 190.6° during the next southern spring. The location is 81.9°S, 4.75°E. (right) Outlined crack pattern and point sources (circles) of both images. The crack pattern is significantly different in the second year, as well as positions of point sources. The difference in scale of the pattern can be explained by the difference in L_s.

orientation is determined by the local wind direction at the time of fan formation. In Figure 7b, one can see the development of the first cracks. At the same time most of the fans seem to disappear and only their sources are still visible. The cracks are situated between these sources. In Figure 7c one can see a further development of the cracks: the area covered by the cracks is considerably darker and larger and the crack density in previously crack-covered areas increases.

[30] In the region of Manhattan-Frontinella (Figure 8, area 1), dark areas of araneiform terrain is affected by early (L_s < 200°) localized jet activity. They show the standard behavior of continuous brightening and then progressive defrosting. In area 2 we observed an episode of late (L_s = 230°–240°) fan activity in an already brightened area. In this case of late activity, the sources of the surface dark deposits seem to be aligned along linear segments, i.e., cracks, which is not the case for the fans in area 1. The fact that crack-related activity is happening at a later L_s than the localized activity fits to the above discussed influence of small scale topography: it promotes early jet activity and prevents the creation of a continuous rigid slab ice sheet that can exhibit cracks.

[31] We also observe the two types of jet activity in HiRISE images acquired in the region of Starfish (Figure 9). As in Manhattan, the jet activity associated with the polygonal cracks affects the smoother terrain whereas the rougher terrain is affected by the localized jet activity. However, in contrast to Manhattan, the jet activity associated with the dark polygons in the smooth flat terrain appears early (between L_s = 183° and L_s = 199°) and most of the localized jet activity later (between L_s = 199° and L_s = 205°). The general topography of this region (Figure 9a) could explain this timing: the smooth terrain where we see the earlier activity is flat whereas the rougher terrain where we detect a later localized jet activity corresponds to a pole-facing slope with an average slope ranging between 2 and 3°. This difference in the slope leading to the difference in the incident solar energy is probably enough to explain the difference in the time of crack initialization. Our modeling of the distribution of incident solar energy and consequent ice breaking stresses in this region supports this hypothesis. It is described in the next section. Contrasting with the case of Starfish, there is no strong difference of slope between the smooth and the rough area in Manhattan (Figure 8).

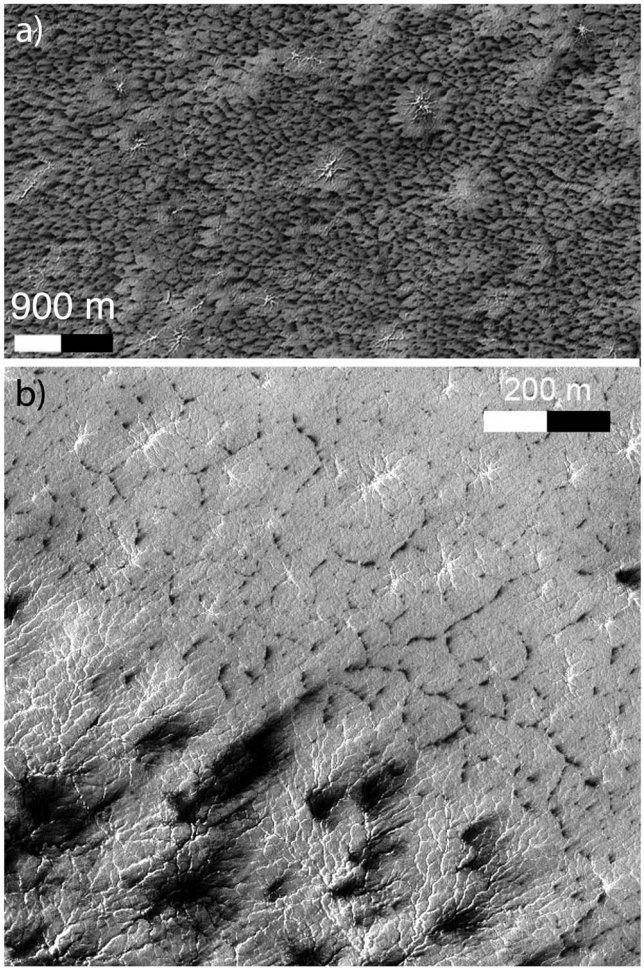

Figure 6. Interaction of the cracks with substrate features - araneiforms. The cracks do not form over araneiforms. Images (a) PSP-003720-0930, location 87.1°S, 126.2°E and (b) ESP-012821-0865, at 86.2°S, 99.1°E.

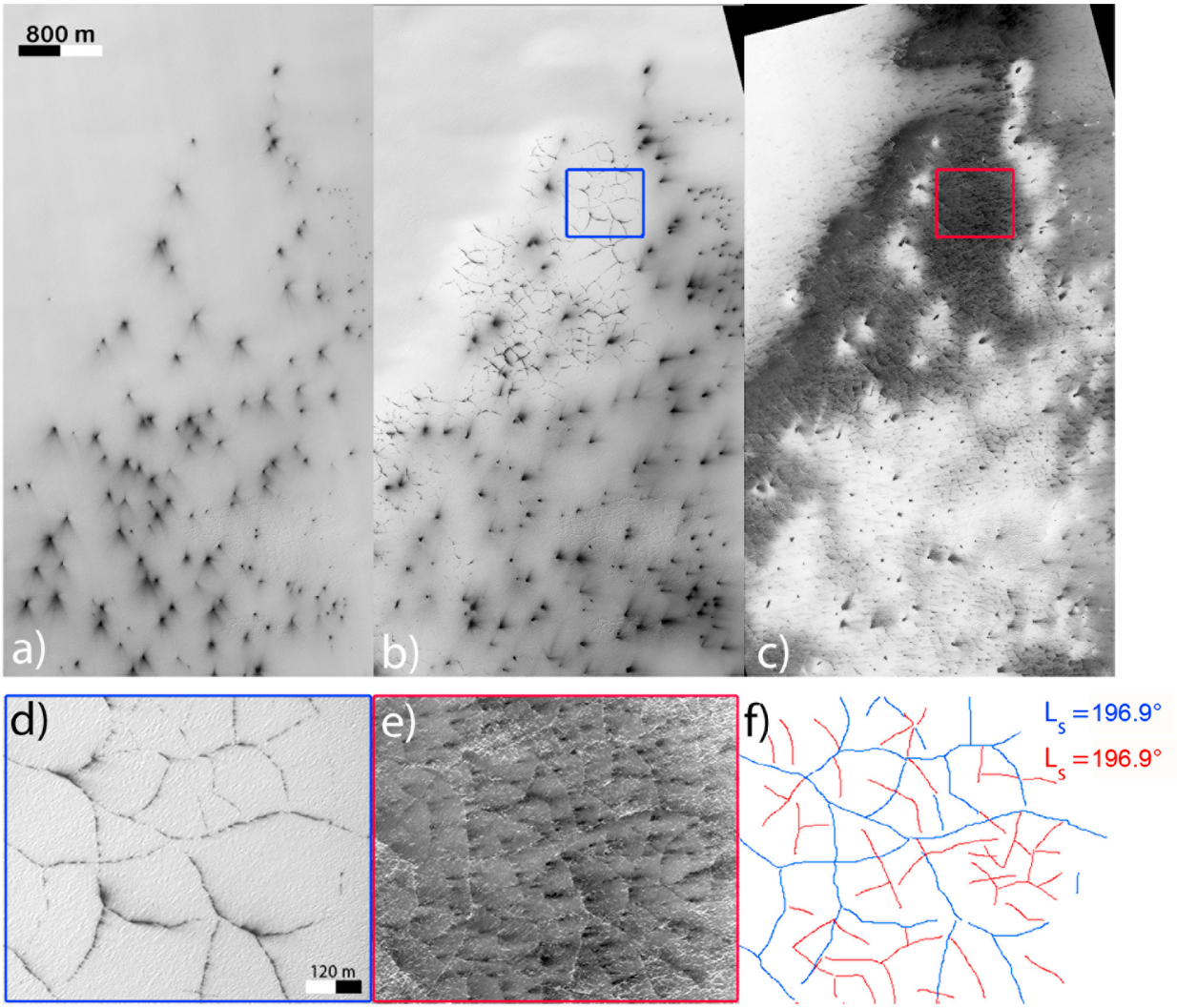

Figure 7. An example of evolution of the cracks during spring from (a) L_s = 190.6° to (b) L_s = 196.6° and to (c) L_s = 216.4° at the location lat = 81.9°S, lon = 4.8°E (non-cryptic terrain); (d) A close sub-frame from Figure 7b, the position of this sub-frame is outlined in blue in Figure 7b; (e) A close sub-frame from Figure 7c, the position of this sub-frame is outlined in red Figure 7c; (f) Crack outlines at L_s = 196.6° (blue) and L_s = 216.4° (red). One can see that from L_s = 196.6° to L_s = 216.4° the cracks spread to a larger area and their scale decreased.

[32] Note that the relationships between terrain texture and general topography might be quite complex. Because of the structure of the Polar Layered Deposits, layers with different composition (i.e., water ice/rock ratio) and surface texture (meter or sub-meter topography) and thus different rheological properties also usually correspond to the different values of slope because of active differential erosion. Therefore, the relative influence of small-scale and large-scale topography might not always be easy to distinguish leading to the strong local variability in the timing and properties of the jet activity.

3. Simulations of Creation of the Cracks in the CO_2 Slab Ice by Breaking

[33] We used a model described by *Portyankina et al.* [2010] to estimate the timing when the ice layer is broken by the pressure growing underneath it. The main features of the model and several improvements made specifically for the present paper are listed below. For the exact mathematical formulation the reader is referred to the work of *Portyankina et al.* [2010]. The model includes the following components:

[34] 1. Calculation of the energy deposited in the lower boundary of the ice layer. This depends on:
(1) Mars's orbital position and the height of the Sun above the local horizon.
These were calculated using the SPICE system (provided by NAIF/JPL) for the times of respective HiRISE observations. This allows the correct calculation of azimuth as well as inclination of the Sun;
(2) the inclination of the local surface toward the instantaneous Sun position.

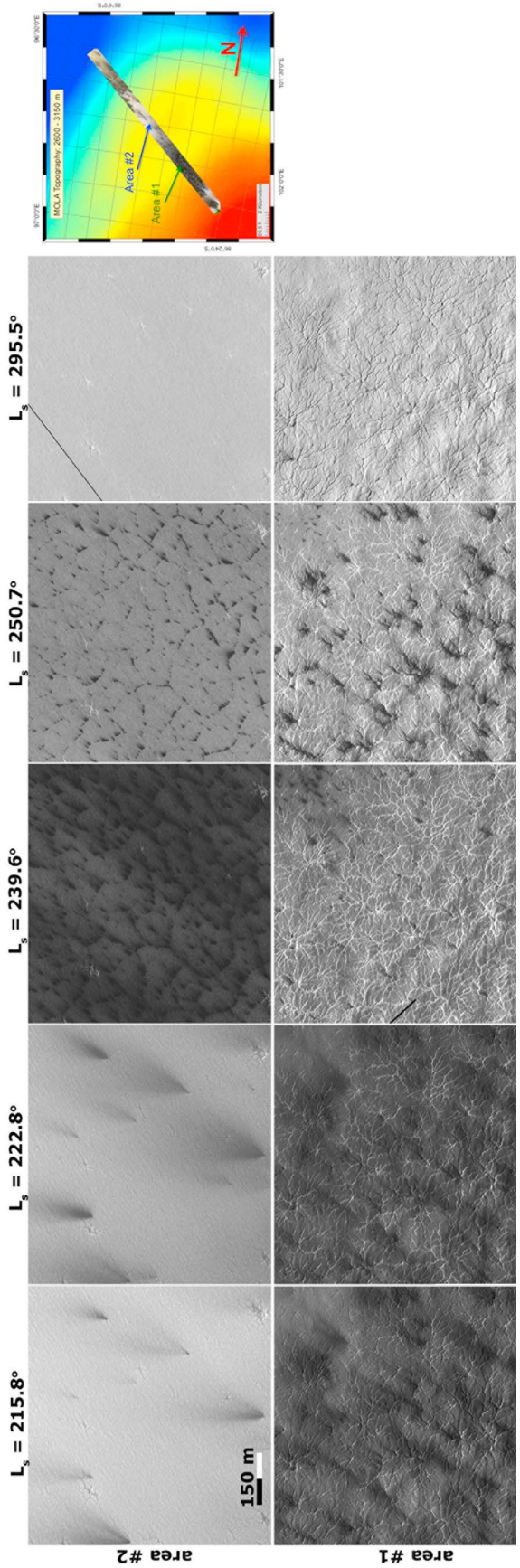

Figure 8. Manhattan-Frontinella region (lat = 86.3°S, lon = 99.2°E). Two episodes of jet activity are observed. The first one, starting in early spring (before L_s = 215°) results in the deposition of dust fans in areas where bright channels are observed (area 1). Later in spring, around L_s = 240°, a second episode of jet activity affects a smooth bright area previously only tenuously disturbed by these processes (area 2). Contrary to area 1, the jet activity is located along linear fractures or the cracks in the CO_2 slab layer.

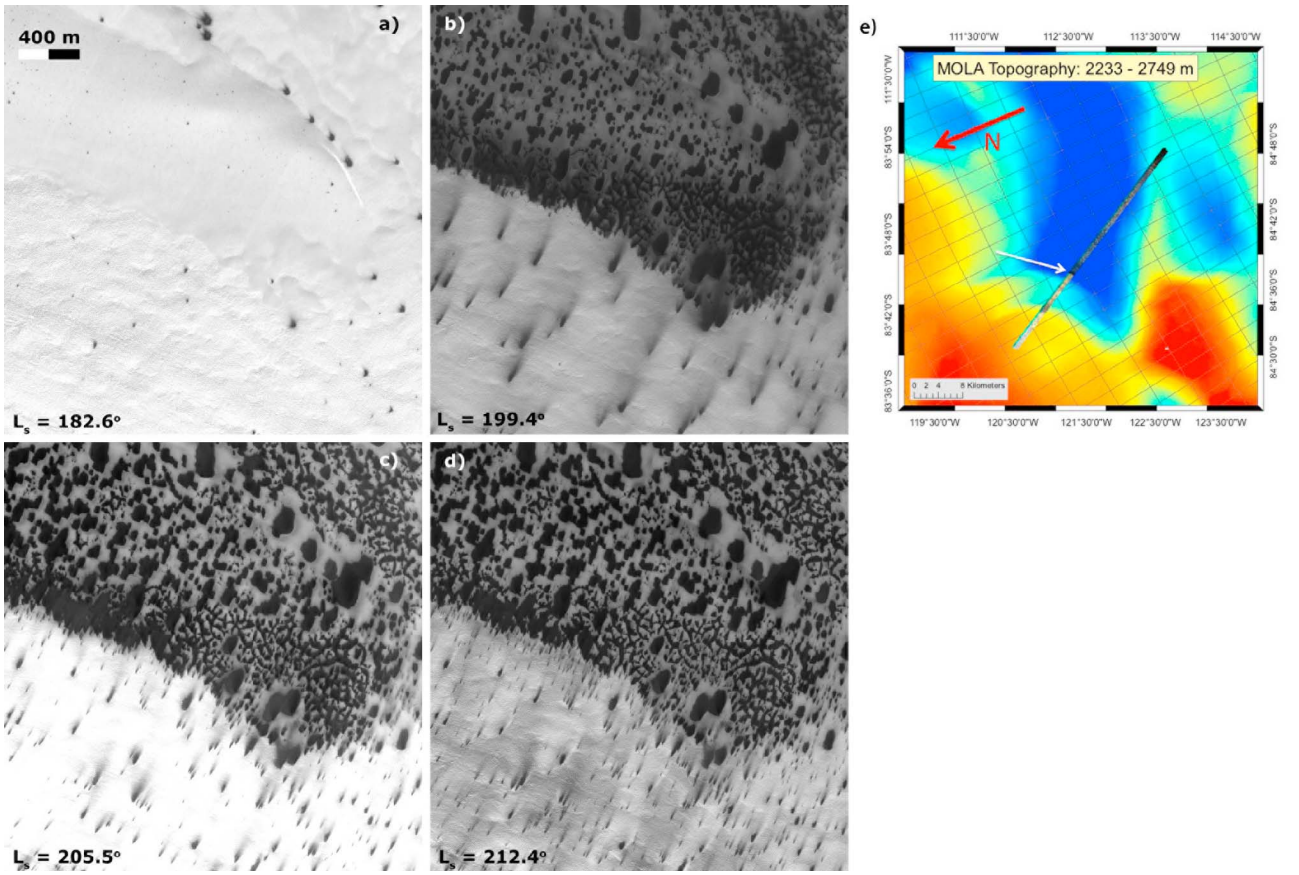

Figure 9. The region of Starfish (−84.3°S, 242.1°E) as seen by HiRISE. As in the case of Manhattan Frontinella, we observe two different kinds of jet activity, localized and associated with polygonal cracks that affect a rough and a smooth terrain, respectively. However, contrary to the previous case, the polygonal jet activity occurs earlier than the massive localized jet activity, certainly because the rough terrain showing localized activity is on a pole-facing slope and receives less solar energy in early spring. Subframes from HiRISE images PSP-002567-0955, PSP-002936-0955, PSP-003068-0955, PSP-003213-0955 are used.

This part of the model was improved compared to the version given by *Portyankina et al.* [2010]. Here MOLA elevation maps are used to calculate the local solar incidence angle and if the area is shadowed by the topography nearby. It is performed using a simple ray tracing algorithm. This improvement allows more correct consideration of the energy distribution on the surface making it possible to distinguish between the shadowed and the sunlit areas inside one HiRISE image at any point in time. This will lead to a better understanding if different appearances and behavior of neighboring areas can be explained by the differences in rate and timing of their insolation;

(3) the optical depth of the Martian atmosphere. As shown by *Vincendon et al.* [2008], in the Martian circumpolar areas during local spring, the atmospheric opacity may very significantly. Unfortunately there is no measurement of optical opacity at the times considered in our model, but the closest in time observations (at L_s = 221°) show very low values of optical depth <0.15. In the present paper for the sake of simplicity we used a constant value of optical opacity equal to 0.1.

(4) the CO_2 ice sheet optical properties (reflectance and absorbance) and its thickness. In these calculations, the CO_2 slab is treated as a continuous media with optical properties normally used for CO_2 ice (albedo = 0.7, emissivity of 0.36) and corresponding optical depth of 0.45 to represent non negligible contamination of ice by atmospherically precipitated dust. The thickness of the sheet is calculated accordingly to the sublimation rate;

[35] 2. Calculation of the pressure growing underneath the flat ice plate in response to the ice sublimation from the lower plate surface.

Using the outputs from the previous sub-model we can calculate the sublimation flux of the CO_2 ice from the lower boundary of the ice layer and hence, the pressure in the sub-ice cavity. This is calculated using the ideal gas equation. The only free parameters here are the boundary conditions relating to volume and pressure under the ice at the beginning of sublimation. The permeability of the underlying substrate to gas molecules translates into the volume available for gas expansion underneath the ice sheet. We considered the permeable layer to be 20 cm deep representing desiccated regolith layer.

[36] 3. Calculation of the stress that is induced by the pressure in the ice plate.

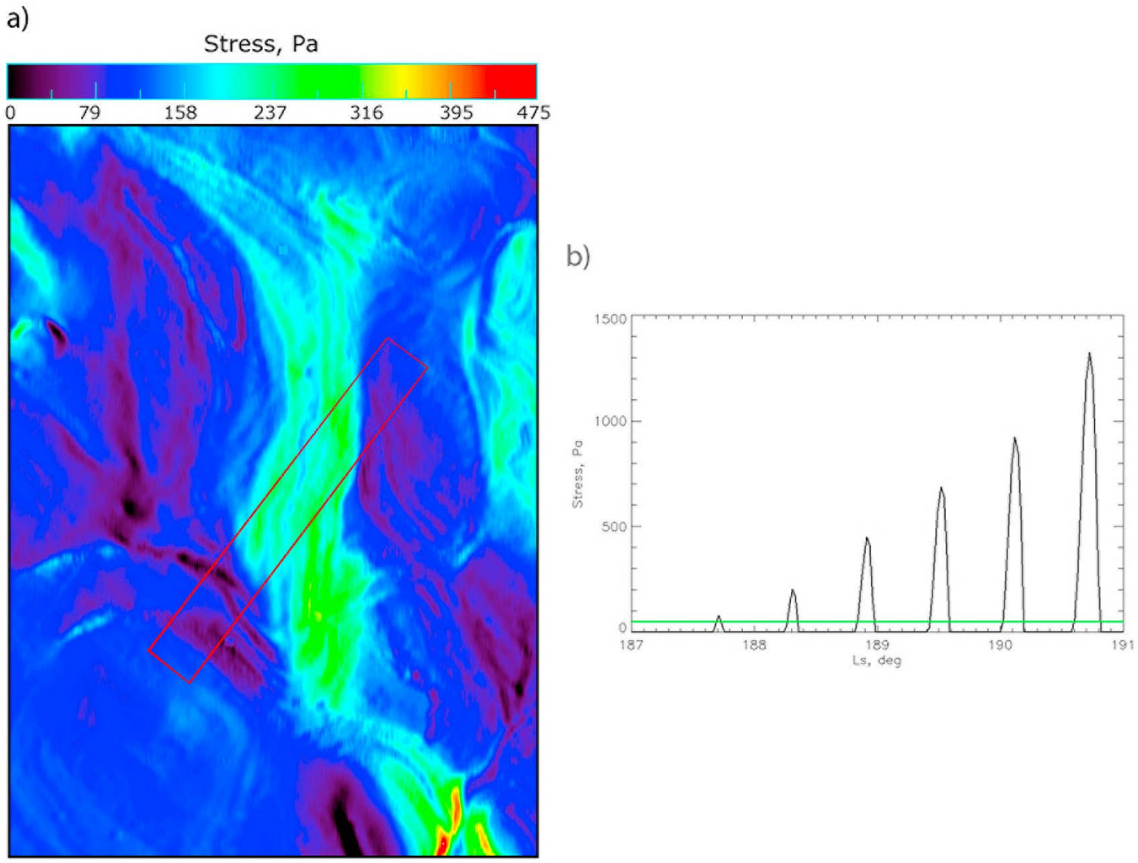

Figure 10. Stress produced in the ice layer by pressure growing underneath. (a) Color map of stress in the ice at L_s = 188° at local noon. Red rectangle indicates the position of HiRISE image PSP-002567-0955. (b) Stress at the position of the cracks as function of time (season and sol). Green line indicates the lowest flexural strength of water ice.

The pressure growing with time puts a stress on the ice plate and eventually will burst it. If we assume the geometry of the plate (for example, circular plate with simply supported edges) and the pressure distribution under the plate (the simplest case is uniform pressure over some circular area, no pressure outside this area) then we can estimate the stress, induced in the plate by this pressure. We used an engineering approach for the calculation of stability of plates and shells described by *Ugural* [1998] where stress is provided as the solution of a differential equation relating the size of a plate, pressure load on it and the mechanical properties of the plate material. As an outcome of this calculation we get a distribution of the stress over the plate for each point in time. Comparing the maximum stress over the plate to the flexural strength (known also as modulus of rupture) of CO_2 ice one is able to define the moment when the plate breaks. Unfortunately, the measurements of flexural strength of CO_2 ice are absent. We used water ice flexural strength instead. From the coring experiments [*Garry and Wright*, 2004] it is known that for coring of CO_2 ice one needs more power than for coring of water ice. It presumes that CO_2 ice is stronger than water ice, but even so it can still be more fragile for fracturing.

This part of the model in its present shape is highly uncertain mostly because of lack of measurements of the mechanical properties of CO_2 ice. The stress distribution in the ice plate under the load of subliming gas depends on the Young's modulus and Poisson's ratio of the plate material. This is unknown for the CO_2 slab ice. For the calculations here we used the values for water ice. Other undefined parameters of this part are the size of the ice sheet that is able to bend and the area that is exposed to the pressure load. This is highly dependent on the small scale topography of the considered area. Local trenches and hills provide a limitation to the creation of the rigid horizontal ice layer. They also create shadowed cold traps for CO_2. We used the average size of the cracks in each area as an indication of the size of a plate that can be bent.

[37] As one example we discuss here the creation of the cracks in the Starfish region. The region is shown in Figure 9. From these observations we conclude that some small and very localized activity happened before L_s = 182° (most probably related to the small scale topography) while the episode of higher activity that led to the creation of the crack network happened between L_s = 182° and L_s = 199°. Our calculation of the stress that is produced in the ice sheet in this area is shown in Figure 10. Figure 10a shows a color map of stress in the area around HiRISE image position (PSP-002567-0955 in this case) at local noon. This is the time when the ice gets the highest solar radiation input. One

can see that the crack-affected areas exhibit much higher values of the stress compared to the areas of no (or only small and localized) activity. This relation does change depending on the time of day. For example, in the early morning slopes facing east get most of the insolation. However in this early season early morning sunlight gets strongly absorbed and scattered in the atmosphere leaving insufficient energy for ice fracture. The very localized activity that we see in those areas must be related to the small scale topography that provides additional inclination toward the sun. However the main activity happens in the areas that are illuminated during maximum diurnal solar energy input, in this particular case - the smooth area of the cracks formation. Our calculations show that breaking of the ice layer is possible starting from L_s = 188°. As one can see in Figure 10a, before this time the pressure underneath the ice layer is not strong enough to create stress in the plate that is larger than even the lowest flexural strength of water ice (50 Pa - measured for water ice with soil inclusions and air bubbles) and far too small for the highest value of the water ice flexural strength (10^5 Pa, i.e., outside the vertical axes scale of the plot). As we believe that the CO_2 ice rigidity lies somewhere inside those extreme values for water ice, the break-up of the ice in this area should happen some time starting from L_s = 188°. This fits well the HiRISE observations of the area.

4. Conclusions

[38] In summary the main characteristics of seasonal crack networks are: (1) they are observed in north and south polar areas during local spring and only during restricted periods of time; (2) cracks disappear in summer and appear again in the subsequent spring in the same locations; (3) their orientations and sizes are changing from year to year; (4) cracks are more common on flat smooth substrates and typically form in the presence of the movable material; and (5) they were not observed overlying araneiforms or etched polygons. These observations support the hypothesis that cracks are formed in a seasonal ice layer which disappears completely in summer and forms again in the subsequent winter, and are unrelated to polygonal cracks in the substrate. Hence observed cracks indicate a layer of semi-translucent material that is not directly observed by other instruments. The polygonal cracks are distinctive features of both polar areas during local spring. They were observed in many separate locations. It is reasonable to conclude that the CO_2 slab layer almost completely covers polar areas at least at some periods of local spring.

[39] The observation that cracks form in a direct vicinity to araneiforms but never overlie them indicates that araneiforms are not the direct products of cracks but they are related via the process of basal sublimation of CO_2 ice layer that creates both structures. The highly variable topography of araneiforms most probably prevents formation of cracks and favors the creation of localized vents. We observe that at least some erosion of the substrate happens underneath cracked ice layer because of fans of dark material on top of it. It might be that only a very thin layer of airborne dust gets recycled every year via cracks and the bulk of the substrate stays intact because of its high resistance to the erosion. Alternatively, it might be that underneath the cracked ice we observe the creation of the very first depressions that will with time result in araneiform structures.

[40] The timing of the appearance of the cracks is consistent with fracturing of CO_2 ice by gas pressure from below. Our model supports the idea that the ice fracturing can occur early in spring at the time when the cracks are observed to appear. In this context the eruptions of jets (and hence the location of fans) would seem less likely to stem from point-like vent sources than from cracks, because a clear body of ice is expected to break in elongated fractures (i.e., cracks) rather than create vents confined to a small area (<0.1 m^2). One explanation for the abundance of vent sources could be that a number of them are actually cracks where most of the elongated fracture is very clean and not detectable by the existing instruments and the vent made visible by eruption of localized dark substrate material. Additionally, jets can come from vents that are unrelated to cracks but are instead formed at localized weak spots in the ice. These weak spots are expected to form when the ice covers terrain with highly variable topography, for example over araneiform terrain. This is supported by the general observation that araneiform terrains are associated only with activity from confined vents and so far no cracks were observed on top of them.

[41] Important parameters of the rheological properties of the CO_2 compact ice and snow under temperature and pressure representative for Mars remain poorly constrained. These are very important for our model and can dramatically change its outcome. They should be experimentally determined and incorporated in future developments of this work.

[42] **Acknowledgments.** This research was supported by the Swiss National Science Foundation.

References

Appere, T., B. Schmitt, Y. Langevin, S. Doute, A. Pommerol, F. Forget, A. Spiga, B. Gondet, and J.-P. Bibring (2011), Winter and spring evolution of the northern seasonal deposits on Mars from OMEGA on Mars Express, *J. Geophys. Res.*, *116*, E05001, doi:10.1029/2010JE003762.

Brown, A. J., W. M. Calvin, P. C. McGuire, and S. L. Murchie (2010), Compact Reconnaissance Imaging Spectrometer for Mars (CRISM) south polar mapping: First Mars year of observations, *J. Geophys. Res.*, *115*, E00D13, doi:10.1029/2009JE003333.

Cornwall, C., and T. N. Titus (2010), A comparison of Martian north and south polar cold spots and the long-term effects of the 2001 global dust storm, *J. Geophys. Res.*, *115*, E06011, doi:10.1029/2009JE003514.

El Maarry, M. R., W. J. Markiewicz, M. T. Mellon, W. Goetz, J. M. Dohm, and A. Pack (2010), Crater floor polygons: Desiccation patterns of ancient lakes on Mars?, *J. Geophys. Res.*, *115*, E10006, doi:10.1029/2010JE003609.

Garry, J. R. C., and I. P. Wright (2004), Coring experiments with cryogenic water and carbon dioxide ices–toward planetary surface operations, *Planet. Space Sci.*, *52*(9), 823–831, doi:10.1016/j.pss.2004.03.003.

Hansen, C. J., N. Thomas, G. Portyankina, A. McEwen, T. Becker, S. Byrne, K. Herkenhoff, H. Kieffer, and M. Mellon (2010), HiRISE observations of gas sublimation-driven activity in Mars southern polar regions: I. Erosion of the surface, *Icarus*, *205*, 283–295, doi:10.1016/j.icarus.2009.07.021.

Hansen, C. J., et al. (2011), Seasonal erosion and restoration of Mars northern polar dunes, *Science*, *331*, 575–578, doi:10.1126/science.1197636.

Hansen, G. B. (1997), The infrared absorption spectrum of carbon dioxide ice from 1.8 to 333 μm, *J. Geophys. Res.*, *102*, 21,569–21,588, doi:10.1029/97JE01875.

Hansen, G. B. (2005), Ultraviolet to near-infrared absorption spectrum of carbon dioxide ice from 0.174 to 1.8 μm, *J. Geophys. Res.*, *110*, E11003, doi:10.1029/2005JE002531.

Kieffer, H. H. (2007), Cold jets in the Martian polar caps, *J. Geophys. Res.*, *112*, E08005, doi:10.1029/2006JE002816.

Kieffer, H. H., T. N. Titus, K. F. Mullins, and P. R. Christensen (2000), Mars south polar spring and summer behavior observed by TES: Seasonal cap evolution controlled by frost grain size, *J. Geophys. Res.*, *105*, 653–9700, doi:10.1029/1999JE001136.

Langevin, Y., J.-P. Bibring, S. Douté, M. Vincendon, F. Poulet, B. Gondet, B. Schmitt, F. Forget, F. Montmessin, and Omega Team (2006), CO_2 ice and H_2O ice in the seasonal caps of Mars during the spring retreat phase, *LPI Contrib. 1323*, p. 8091, Lunar and Planet. Inst., Houston, Tex.

Leighton, R. B., and B. C. Murray (1966), Behavior of carbon dioxide and other volatiles on Mars, *Science*, *153*, 136–144, doi:10.1126/science.153.3732.136.

Levy, J. S., J. W. Head, and D. R. Marchant (2009), Thermal contraction crack polygons on Mars: Classification, distribution, and climate implications from HiRISE observations, *J. Geophys. Res.*, *114*, E01007, doi:10.1029/2008JE003273.

Levy, J. S., D. R. Marchant, and J. W. Head (2010), Thermal contraction crack polygons on Mars: A synthesis from HiRISE, Phoenix, and terrestrial analog studies, *Icarus*, *206*, 229–252, doi:10.1016/j.icarus.2009.09.005.

Matsuo, K., and K. Heki (2009), Seasonal and inter-annual changes of volume density of Martian CO_2 snow from time-variable elevation and gravity, *Icarus*, *202*, 90–94, doi:10.1016/j.icarus.2009.02.023.

McEwen, A. S., et al. (2007), Mars Reconnaissance Orbiterś High Resolution Imaging Science Experiment (HiRISE), *J. Geophys. Res.*, *112*, E05S02, doi:10.1029/2005JE002605.

Mellon, M. T. (1997), Small-scale polygonal features on Mars: Seasonal thermal contraction cracks in permafrost, *J. Geophys. Res.*, *102*, 25,617–25,628, doi:10.1029/97JE02582.

Osterloo, M. M., F. S. Anderson, V. E. Hamilton, T. D. Glotch, A. M. Baldridge, P. R. Christensen, J. L. Bandfield, and L. L. Tornabene (2007), Discovery and distribution of chloride-bearing deposits in the ancient cratered terrain of Mars from THEMIS, *Eos Trans. AGU*, *88*(52), Fall Meet. Suppl., Abstract P13D-1563.

Pilorget, C., F. Forget, E. Millour, M. Vincendon, and J. B. Madeleine (2011), Dark spots and cold jets in the polar regions of Mars: New clues from a thermal model of surface CO_2 ice, *Icarus*, *213*, 131–149, doi:10.1016/j.icarus.2011.01.031.

Piqueux, S., and P. R. Christensen (2008), North and south subice gas flow and venting of the seasonal caps of Mars: A major geomorphological agent, *J. Geophys. Res.*, *113*, E06005, doi:10.1029/2007JE003009.

Piqueux, S., S. Byrne, and M. I. Richardson (2003), Sublimation of Mars's southern seasonal CO_2 ice cap and the formation of spiders, *J. Geophys. Res.*, *108*(E8), 5084, doi:10.1029/2002JE002007.

Pommerol, A., G. Portyankina, N. Thomas, K.-M. Aye, C. J. Hansen, M. Vincendon, and Y. Langevin (2011), Evolution of south seasonal cap during Martian spring: Insights from high-resolution observations by HiRISE and CRISM on Mars Reconnaissance Orbiter, *J. Geophys. Res.*, *116*, E08007, doi:10.1029/2010JE003790.

Portyankina, G., W. J. Markiewicz, N. Thomas, C. J. Hansen, and M. Milazzo (2010), HiRISE observations of gas sublimation-driven activity in Mars southern polar regions: III. Models of processes involving translucent ice. *Icarus*, *205*, 311–320, doi:10.1016/j.icarus.2009.08.029.

Schmidt, F., B. Schmitt, S. Douté, F. Forget, J.-J. Jian, P. Martin, Y. Langevin, J.-P. Bibring, and the OMEGA Team (2010), Sublimation of the Martian CO_2 seasonal south polar cap, *Planet. Space Sci.*, *58*, 1129–1138, doi:10.1016/j.pss.2010.03.018.

Smith, D. E., M. T. Zuber, and G. A. Neumann (2001), Seasonal variations of snow depth on Mars, *Science*, *294*, 2141–2146.

Thomas, N., C. J. Hansen, G. Portyankina, and P. S. Russell (2010), HiRISE observations of gas sublimation-driven activity in Mars southern polar regions: II. Surficial deposits and their origins, *Icarus*, *205*, 296–310, doi:10.1016/j.icarus.2009.05.030.

Thomas, N., G. Portyankina, C. J. Hansen, and A. Pommerol (2011), Subsurface CO_2 gas flow in Mars's polar regions: Gas transport under constant production rate conditions, *Geophys. Res. Lett.*, *38*, L08203, doi:10.1029/2011GL046797.

Ugural, A. C. (1998), *Stresses in Plates and Shells*, 2nd ed., 528 pp., McGraw-Hill Sci., Boston.

van Gasselt, S., D. Reiss, A. K. Thorpe, and G. Neukum (2005), Seasonal variations of polygonal thermal contraction crack patterns in a south polar trough, Mars, *J. Geophys. Res.*, *110*, E08002, doi:10.1029/2004JE002385.

Vincendon, M., Y. Langevin, F. Poulet, J.-P. Bibring, B. Gondet, D. Jouglet, and OMEGA Team (2008), Dust aerosols above the south polar cap of Mars as seen by OMEGA, *Icarus*, *196*, 488–505, doi:10.1016/j.icarus.2007.11.034.

K.-M. Aye, A. Pommerol, G. Portyankina, and N. Thomas, Physikalisches Institut, University of Bern, Bern CH-3012, Switzerland. (aye@space.unibe.ch; pommerol@space.unibe.ch; portyankina@space.unibe.ch; thomas@space.unibe.ch)

C. J. Hansen, Planetary Science Institute, Tucson, AZ 85719-2395, USA. (cjhansen@psi.edu)